Available online at www.sciencedirect.com

ScienceDirect

Journal of the European Ceramic Society 34 (2014) 1131–1138

www.elsevier.com/locate/jeurceramsoc

Fabrication of cylindrical SiC_f/Si/SiC-based composite by electrophoretic deposition and liquid silicon infiltration

Alberto Ortona [a], Thomas Fend [b], Hyun-Woo Yu [c], Kati Raju [c], Dang-Hyok Yoon [c,*]

[a] *ICIMSI, SUPSI, Galleria 2, CH-6928 Manno, Switzerland*
[b] *Institute of Solar Research, German Aerospace Center, Linder Höhe, 51147 Köln, Germany*
[c] *School of Materials Science and Engineering, Yeungnam University, Gyeongsan 712-749, Republic of Korea*

Received 6 August 2013; received in revised form 28 October 2013; accepted 29 October 2013
Available online 3 December 2013

Abstract

Cylindrical SiC-based composites composed of inner Si/SiC reticulated foam and outer Si-infiltrated SiC fiber-reinforced SiC (SiC_f/Si/SiC) skin were fabricated by the electrophoretic deposition of matrix particles into SiC fabrics followed by Si-infiltration for high temperature heat exchanger applications. An electrophoretic deposition combined with ultrasonication was used to fabricate a tubular SiC_f/SiC skin layer, which infiltrated SiC and carbon particles effectively into the voids of SiC fabrics by minimizing the surface sealing effect. After liquid silicon infiltration at 1550 °C, the composite revealed a density of 2.75 g/cm^3 along with a well-joined interface between the inside Si/SiC foam and outer SiC_f/Si/SiC skin layer. The results also showed that the skin layer, which was composed of 81.4 wt% β-SiC, 17.2 wt% Si and 1.4 wt% SiO_2, exhibited a gastight dense microstructure and the flexural strength of 192.3 MPa.

Keywords: SiC composites; Electrophoretic deposition; Silicon infiltration

1. Introduction

Because silicon carbide (SiC) exhibits excellent thermochemical stability in severe environments and strength retention to high temperature as well as sufficient thermal conductivity, it has become a prime candidate material for high temperature heat exchanger applications.[1] However, SiC is difficult to be sintered due to the high covalence of Si–C bond and also shows brittle nature, especially with monolithic structures. Therefore, SiC fiber-reinforced SiC composites (SiC_f/SiC) have been proposed to enhance fracture toughness and long-term reliability.[2] Different techniques have been developed to fill the matrix phase into the voids of SiC_f/SiC composites, such as chemical vapor infiltration, polymer impregnation and pyrolysis, liquid silicon (Si) infiltration, slurry impregnation and combinations of these processes.[2–6] Among these, liquid Si infiltration has been demonstrated as a rapid and low-cost composite manufacturing process compared to the other processes.[7] However, the presence of free Si is inevitable with this process, which should be minimized to enhance the heat exchanging property and high temperature stability.[8] To increase the relative content of SiC by decreasing the amount of free Si in the composites, therefore, the pre-infiltration of SiC and carbon powder into a fiber preform would be desirable because the Si melt reacts with carbon in the preform and forms reaction-bonded SiC during the Si infiltration performed at >1420 °C in vacuum.[5]

For the infiltration of matrix particles into the tightly woven fiber preforms, electrophoretic deposition (EPD) was demonstrated as an effective technique.[9] EPD was initially used for the deposition of thick film on a substrate and is commonly employed nowadays in many ceramic fields, including the formation of wear-resistant layer, anti-oxidant coating and the functional layer for microelectronic devices.[10] The mechanism of EPD is that charged colloidal particles dispersed in a liquid medium migrate and deposit onto a conducting substrate of an opposite charge under a DC electric field. The factors influencing on EPD includes the applied electric field, particle size and its concentration in the suspension, zeta potential and electrophoretic mobility of the particles, viscosity of the suspension, dielectric constant of the liquid medium, electrode distance and

* Corresponding author. Tel.: +82 538102561; fax: +82 538104628.
E-mail address: dhyoon@ynu.ac.kr (D.-H. Yoon).

0955-2219/$ – see front matter © 2013 Elsevier Ltd. All rights reserved.
http://dx.doi.org/10.1016/j.jeurceramsoc.2013.10.037

deposition time.[10] Among these, zeta potential is a key factor in EPD, which confers a long-term stability of particle dispersion by electrostatic repulsion forces and determines the direction as well as the migration velocity of particles. In addition, the addition of a small amount of polymeric binder into the suspension is known to enhance the adhesion of matrix phase to the preform and also helps the homogeneous deposition of constituent particles when multi-component system is used.[11] By replacing the substrate electrode to a conducting fiber preform, EPD can offer a fast and simple infiltration of matrix particles into the preform regardless the shape of the preform. Even though there is a barrier associated with EPD owing to the preferential deposit of the matrix particles at the surface of fiber preform without penetrating into the deep voids, which is called surface sealing effect, this could be minimized by performing EPD combined with ultrasonication.[11]

In these overall perspectives, we tried to fabricate a sandwich-structured Si-infiltrated SiC fiber-reinforced SiC (SiC_f/Si/SiC) composite, which is composed of inner Si/SiC foam and outer SiC_f/Si/SiC skin layer, for the first time for high temperature heat exchanger applications. The specific processes used for the preparation of cylindrical samples include the formation of SiC fabric skin layer around the reticulated SiC foam, SiC and carbon particle infiltration into the SiC fabrics by EPD combined with ultrasonication, and Si-infiltration for consolidation of the skin layer. Compared to the current metal-based heat exchangers with the maximum working temperatures up to 800 °C, this advanced SiC-based structure is expected to increase the heat transfer efficiency by a factor of 2–3 with less thermal loss because it enables the operation at >1000 °C.[1,12] Moreover, an integrated sandwich-structure with a reticulated Si/SiC foam inside and an outer SiC_f/Si/SiC skin, which was adopted in this study, would achieve enough mechanical strength, as reported previously.[13] One of the promising application fields of this SiC-based heat exchanger is the solar absorber in concentrating solar power (CSP) technique, which can generate electricity via the direct concentration of the solar radiation to produce steam or hot air for a turbine operation.[14,15] For this application, the composite should maintain high thermal conductivity, mechanical properties for heat and pressure resistances at operating temperatures, and porosity to create large surfaces for convective heat transfer from the inside foam to the fluid.[12] The present paper is focused on the fabrication of a cylindrical SiC_f/Si/SiC composite, while the evaluation on the thermo-physical and heat transfer properties for this sample is under consideration.

2. Experimental procedure

2.1. Starting materials

A reticulated ERBISIC-R (Erbicol SA, Switzerland) produced by a replica method was used as the porous core foam after machining it to a cylindrical shape (20 mm D × 50 mm L). This foam contained ~5 mm sized pores, which is equivalent to 10 ppi (pores per inch), and was made of α-SiC powder in a β-SiC/Si matrix with a density of 2.64 g/cm^3. Two-dimensionally woven Tyranno^{TM}-SA grade-3 fabrics (Ube Industries Ltd., Japan) were used as SiC fabrics for the skin layer, which is known to be stable up to 1500 °C in air and 2200 °C in an inert atmosphere.[16] The fabrics have a 0/90° plain woven structure containing 1600 filaments per yarn. A nano-sized β-SiC (D_m = 52 nm, >97.5% pure, 4620KE, NanoAmor Inc., USA) and carbon black (D_m = 50 nm, >98.5% pure, HiBlack 50L, Shin Woo Materials, Korea) mixture at a 2:1 weight ratio were used as the matrix phase for SiC fabric infiltration. A coarse Si chip (D_m = 2.5 mm, >99.99% pure, Worldex, Korea) was used for Si-infiltration.

2.2. SiC foam wrapping with the SiC fabrics

After cutting the SiC fabrics into a rectangular shape (52 mm × 325 mm), 2 wt% of polysilazane resin (Ceraset PSZ20, Clariant Advanced Materials, Germany) with respect to the fabric weight was pasted onto one side using a brush as an adhesive. This fabric was rolled 5 times around the SiC cylindrical foam and then cured at 150 °C for 2 h under a pressure of 1.5 bars using an autoclave. Pyrolysis was performed at 1000 °C for 5 h in an Ar atmosphere at a heating rate of 2 °C/min.

2.3. Slurry preparation and electrophoretic deposition combined with ultrasonication

To prepare a slurry composed of β-SiC and carbon black particles for matrix phase infiltration into the SiC fabrics, 1.5 g of polyvinyl butyral (PVB, Butvar B-98, Mw = 55,000 g/mole, Solutia, USA) was dissolved in 300 g ethyl alcohol, which contained 1.5 g of a polyester/polyamine co-polymeric cationic dispersant (Hypermer KD1, ICI, UK). After adding 20 g of SiC and 10 g of carbon black powder, the slurry was exposed to ball milling for 24 h using 6 mm SiC balls to ensure particle dispersion.

EPD was performed for the cylindrical sample with an applied voltage of 10 V DC for 1 h under the application of 10 W ultrasonic pulses at 60 Hz for the first 50 min to minimize the surface sealing effect. Before performing EPD, the SiC core foam was filled with a wax melt to prevent matrix phase deposition inside foam surface. The distance between the SiC fabric and the stainless steel electrode was 25 mm. After removing the wax filled in the cylindrical sample at 80 °C in air, binder burn-out was performed at 350 °C for 2 h in a N_2 atmosphere.

2.4. Silicon infiltration

After binder burn-out, Si-infiltration was performed at 1550 °C for 30 min under a pressure of 10^{-2} mbar. The sample was placed on boron nitride painted graphite wicks to drain the excess molten Si. Ten grams of Si chips were placed on top of the cylindrical sample, which was a much greater amount than needed to react with the infiltrated carbon black and fill the remaining pores in the skin, based on a preliminary test results.

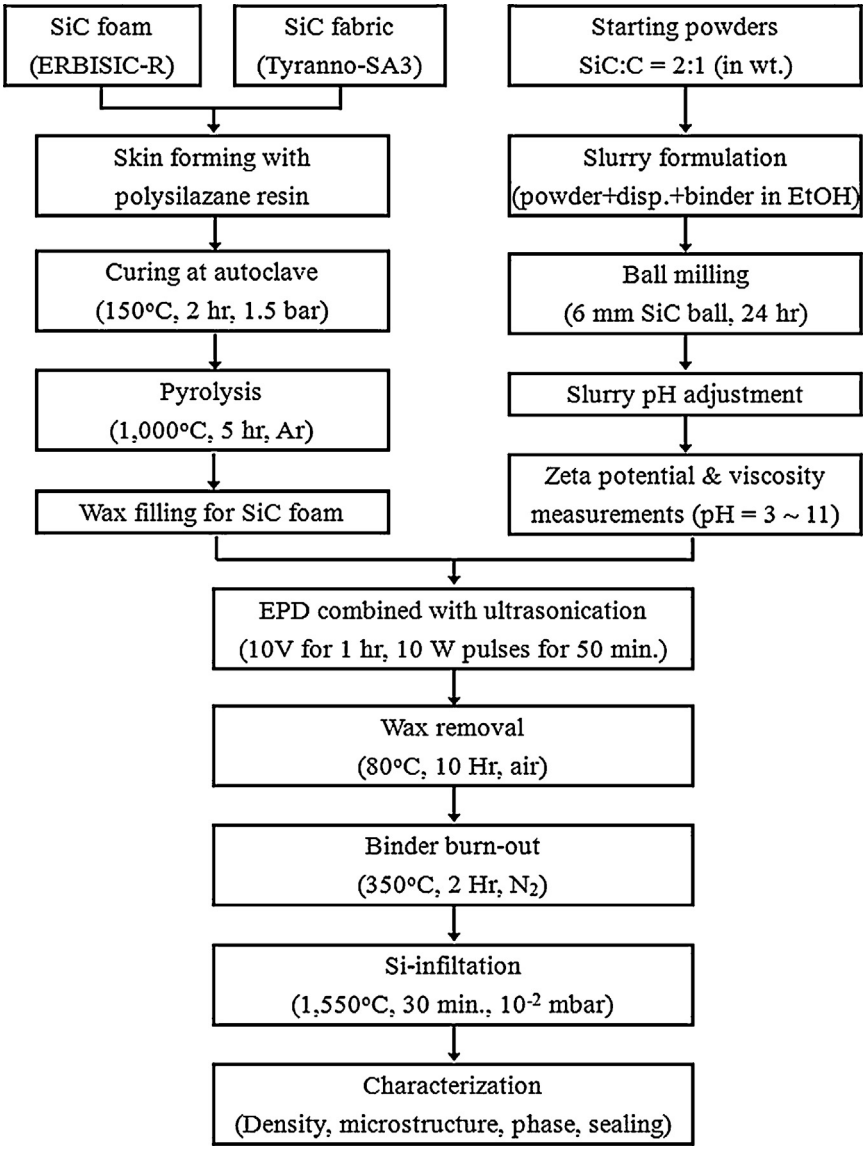

Fig. 1. Schematic diagram of the experimental procedure for the fabrication of sandwich-structured Si/SiC-based composite tube for concentrating solar absorber applications.

2.5. Characterization

Samples were characterized by a variety of techniques. The zeta potentials of SiC and carbon black suspensions in ethyl alcohol containing dispersant were measured using an electroacoustic-type zeta potential analyzer (Zeta Probe, Colloidal Dynamics, USA) for 5 times with an interval of 60 s after adjusting the operational pH of the suspension with NH_4OH and HCl. The viscosity of slurry was also measured at 20 °C using a computer-controlled viscometer (DV-II + Pro, Brookfield, MA, USA) equipped with a small sample adapter with SC4-18 spindle at various shear rates.

The morphology of the starting materials and consolidated bodies were observed by scanning electron microscopy (SEM: S-4800, Hitachi at 15 kV and 10 μA) and high-resolution transmission electron microscopy (HR-TEM: Tecni G2F20 S-twin, FEI operated at 200 keV). The mean particle size of the starting materials was estimated from the SEM/TEM images by measuring the maximum and minimum diameters of 100 grains using image analysis software (SigmaScan, Systat Software, USA). The degree of infiltration for the skin was observed after cryo-fracturing the infiltrated fabric with liquid N_2 followed by SEM. Energy dispersive X-ray spectrometry (EDS: Horiba EX-250) combined with SEM was used to analyze the distribution of each phase after Si infiltration. The density was measured using the Archimedes method, and the phase generated during Si-infiltration was calculated from a Rietveld simulation of the X-ray diffraction (XRD: X'Pert-PRO MPD, PANalytical using Cu Kα line, 40 kV and 30 mA) patterns. After cutting the skin layer into 4 mm × 2 mm × 40 mm pieces, 3-point bending test (UTM AG-50E, Shimadzu, Japan) was performed for 5 samples at a crosshead speed of 0.5 mm/min and a span of 30 mm. Finally a sealing test was performed for the cylindrical composite samples by blowing a compressed air after blocking both ends with a

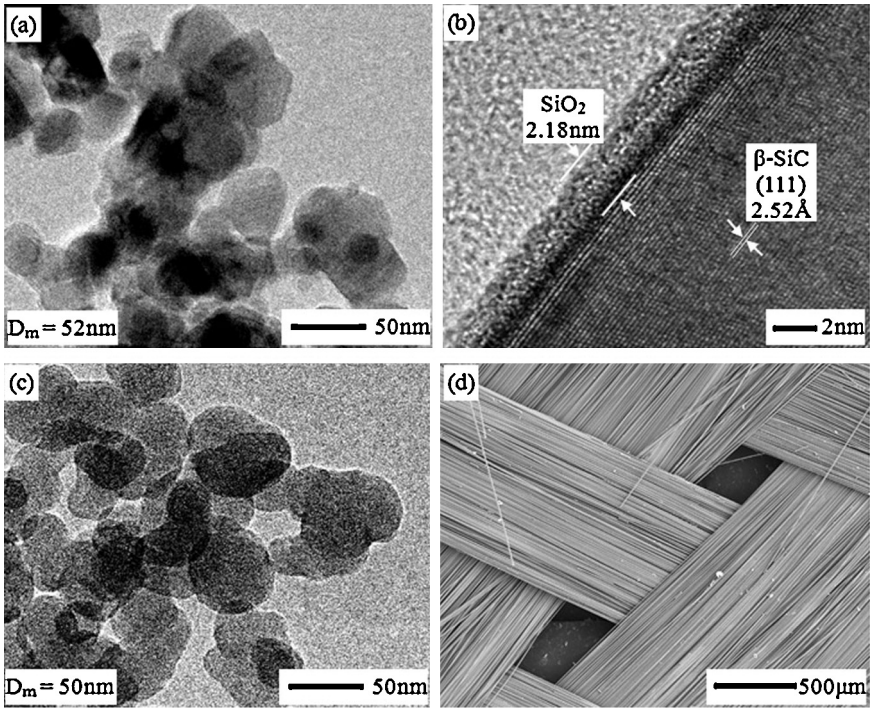

Fig. 2. HR-TEM images of (a), (b) β-SiC and (c) carbon black particles used for the infiltration into the SiC skin fabrics by electrophoretic deposition combined with ultrasonication. SEM image of the Tyranno – SA3 fabric is shown in (d).

wax melt. Fig. 1 shows a schematic diagram of the experimental procedure.

3. Results and discussion

Fig. 2(a–c) shows the HR-TEM images of the β-SiC and carbon black particles, which were used as the matrix phase by infiltrating them into the voids of a SiC fabric for the formation of a SiC_f/Si/SiC skin layer. Because the woven Tyranno fabrics have large inter-bundle voids as well as small intra-bundle gaps between each fiber, as shown in Fig. 2(d), very fine β-SiC and carbon black particles with a mean size of approximately 50 nm were used to enhance infiltration. Moreover, the dispersion of a nano-sized powder, which has a strong tendency for agglomeration, was maximized by adopting the previous systematic research results using the same β-SiC particles.[6,11,17,18] Despite the small particle size, the β-SiC particles had a highly crystalline cubic structure with an inter-planar distance of 2.52 Å, corresponding to the most preferred (1 1 1) orientation [ICSD code: 024171], along with an approximately 2 nm thick SiO_2 layer on the SiC surface, as shown in Fig. 2(b). The formation of the SiO_2 layer on the SiC surface in the presence of O_2 is inevitable from a thermodynamic point of view because the Gibbs formation free energy of SiO_2 is strongly negative, i.e. −785 kJ/mol at room temperature.[19,20] The use of carbon black aims to increase the relative amounts of SiC, which has higher thermal conductivity than Si or C, at the skin layer. SiC is likely to form by a reaction between carbon black and infiltrated-Si at 1550 °C, where the Gibbs free energy for SiC formation from Si and C is −53 kJ/mol.[19,20] The coating of pyrolytic carbon or boron nitride on the SiC fiber for the formation of weak matrix-fiber interface to enhance the damage tolerance was not considered in this feasibility test.[21,22]

Fig. 3 shows the experimental apparatus used for β-SiC and carbon black particle infiltration into the SiC fabric skin by EPD combined with ultrasonication. The apparatus was composed of a positive tubular stainless steel electrode and a negative electrode connected to the cylindrical SiC sample placed in the middle of the chamber. An ultrasonic tip was placed in the slurry, which released 10 W ultrasonic pulses with a 1 second cycle for the first 50 min. These ultrasonic pulses were applied to minimize the surface sealing effect, which inhibits matrix phase infiltration into the deep voids of the fabrics owing to preferential deposition at the fabric surface.[11]

Fig. 4 shows the zeta potential of the SiC and carbon black particles in an ethanol suspension with/without KD1 dispersant as a function of the operational pH. Both particles showed a decrease in zeta potential with increasing the operational pH, regardless the presence of the dispersant, due to the effect of the increased OH^- ions. Moreover, the zeta potential curves for both of SiC and carbon black shifted to higher pH values because KD1 is a cationic dispersant. The iso-electric points (IEPs) of SiC and carbon black without dispersant were 6.37 and 6.90, respectively, while those with dispersant were increased to 8.21 and 7.66, as shown in Fig. 4. Based on this result, the operational pH of the slurry for EPD was set to 4, where both particles have a positive zeta potential. Because the particles tend to migrate to the negative electrode at this condition, the negative electrode was connected to the sample, as shown in Fig. 3. The optimum amount of KD1 dispersant was decided based on the previous sedimentation and rheological results, which was reported elsewhere.[17] The viscosity of the slurry was increased by the

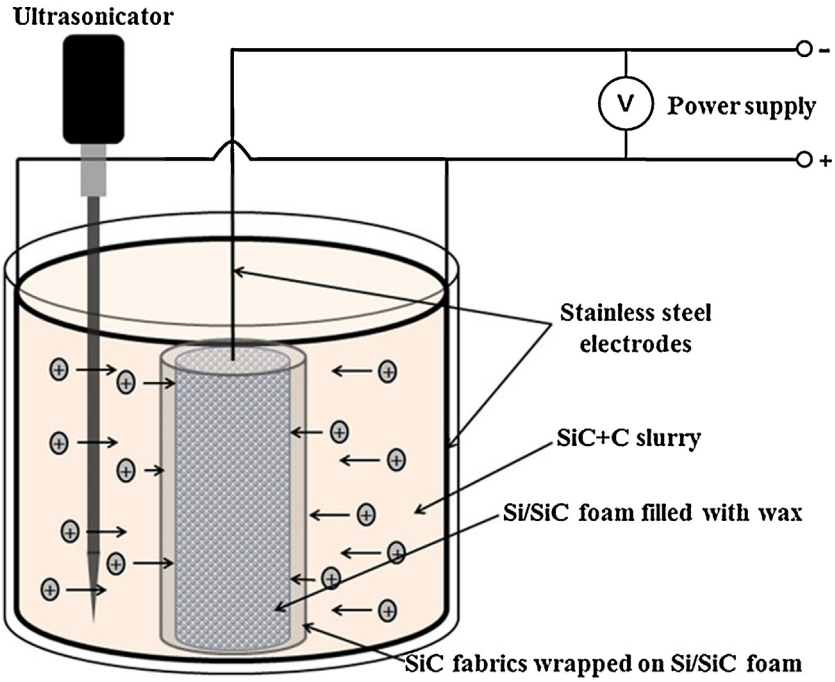

Fig. 3. Schematic diagram of the experimental apparatus used for matrix phase infiltration by electrophoretic deposition combined with ultrasonication.

addition of a 5 wt% PVB binder to minimize the difference in mobility between the 2 types of particles originating from the different zeta potentials. According to the rheological study, the initial viscosity of the suspension was 1.8 mPa s at a fixed shear rate of 26.4 s^{-1}, while that was increased to 3.5 mPa s upon the addition of PVB binder. However, it was found that the addition of PVB binder did not change the zeta potentials of both SiC and carbon black suspensions significantly. The addition of a PVB binder is expected to enhance the adhesion of the matrix phase to the fabric as well as the uniform distribution of each particle, providing steric stabilization of the slurry due to the adsorbed polymeric layer.[10]

Even though the zeta potential of carbon black suspension at an operational pH 4 was low as 15 mV compared to that of SiC (37 mV), it was enough to confer the particle migration based on the preliminary test. Fig. 5(a), (b) and (c) compares the green microstructure of the 1st, 3rd and 5th skin layers, respectively, after matrix phase infiltration using an EPD combined with ultrasonication. The side-view of the infiltrated fabric was also included as an inset for comparison. The matrix phase composed of SiC and carbon black particles appeared to have been infiltrated effectively into the voids of the SiC fabric, even though some unfilled gaps were observed for the 3rd and 5th layers. The application of ultrasonic pulses might be due to this high degree of infiltration, which minimizes the surface sealing effect by releasing the surface adsorbed matrix phase during the EPD process. After 50 min of ultrasonic pulse application for efficient infiltration into the deep voids, EPD without ultrasonication was performed for an additional 10 min to allow surface filling at the final EPD step.

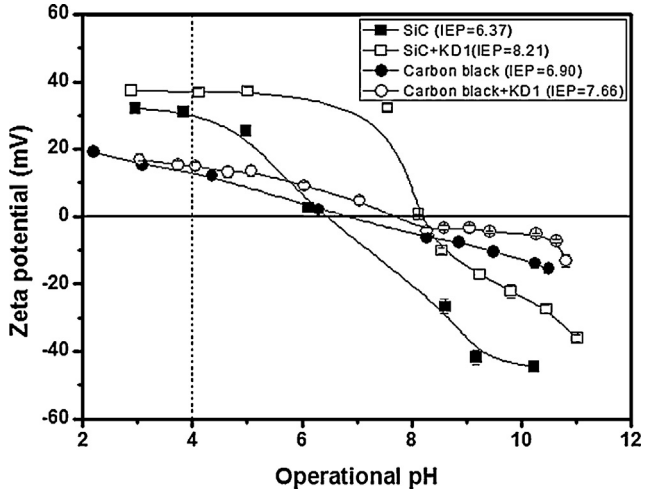

Fig. 4. Zeta potential of the 10 wt% β-SiC and carbon black slurries with/without Hypermer KD1 dispersant as a function of the operational pH in ethyl alcohol.

Fig. 6(a) shows a series of digital camera images of the sample; from the left, the reticulated Si/SiC foam, foam wrapped with SiC fabrics followed by pyrolysis, and the final SiC_f/Si/SiC composite sample. Fig. 6(b) shows the polished surface of the Si-infiltrated sample showing both the foam and skin. The foam in the upper part of the figure contained voids, which are inevitable traces for the foam produced by the replica method,[23] whereas the skin shown in the lower part exhibited a dense morphology. The thickness of skin was found to be approximately 1 mm. The foam and skin joined tightly together without the presence of voids or delamination, which is desirable for conferring high mechanical strength and thermal conduction. The density of the SiC_f/Si/SiC sample was 2.75 g/cm^3, which was higher than that of the as-received SiC foam (2.64 g/cm^3). Although it was difficult to calculate the exact theoretical density for the skin layer owing to its multi-compositions, the skin layer possessed an

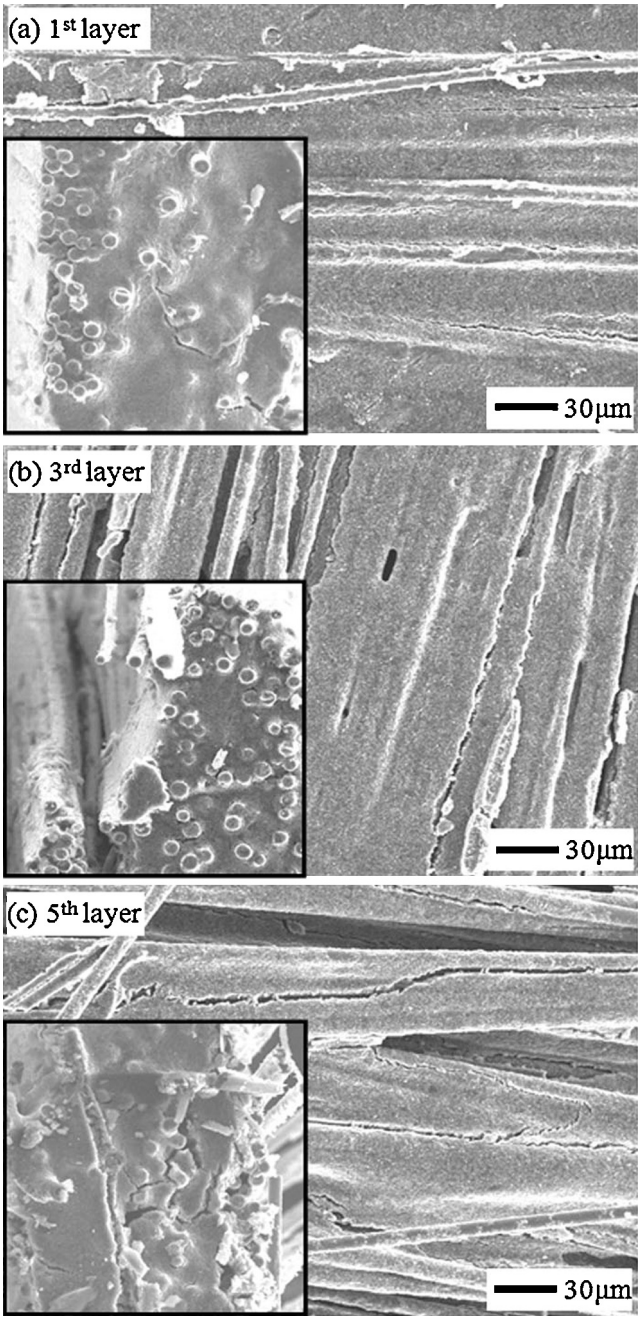

Fig. 5. SEM images of the SiC fabric layer after SiC and carbon black infiltration for (a) 1st, (b) 3rd and (c) 5th layer. The inset shows the side-view of the SiC fabric layer.

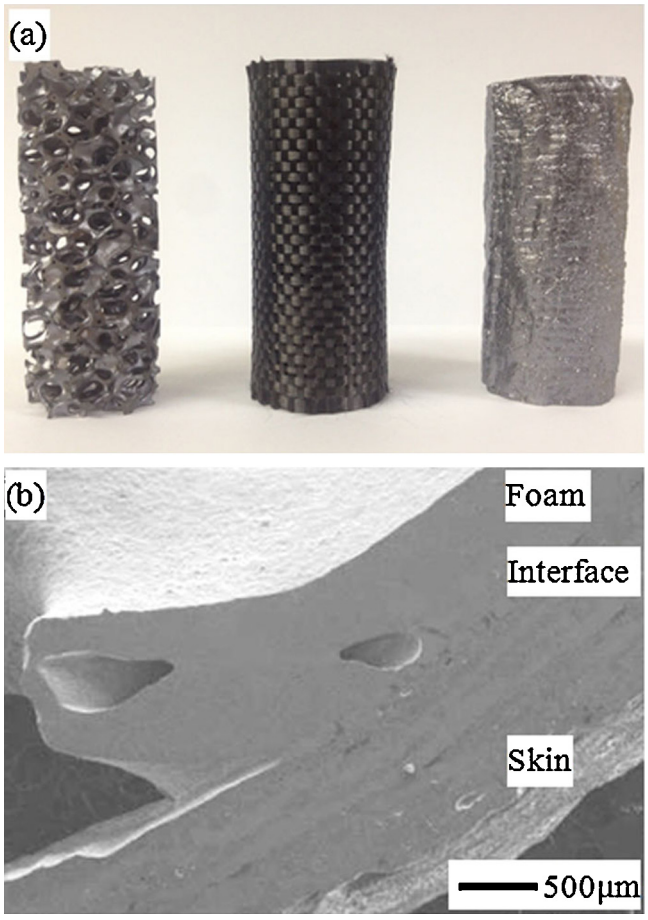

Fig. 6. (a) Digital camera image of the samples: Si/SiC foam, pyrolyzed and Si-infiltrated composite sample (from left), and (b) SEM image of the polished surface containing both the skin and foam region.

ideal microstructure for high temperature heat exchanger applications, including a solar absorber in CSP.

Fig. 7(a), (b) and (c) presents the microstructures of the skin, foam and their interface after Si-infiltration, respectively, with the SEM images for the polished sample. The skin morphology in Fig. 7(a) showed a highly consolidated morphology, indicating the efficient infiltration of SiC and carbon black particles by EPD along with the subsequent Si-infiltration. The round-shaped parts correspond to the SiC fibers with a diameter of 7.5 μm. The foam also showed a dense structure with a large number of SiC precipitates distributed in the Si matrix phase, as shown in Fig. 7(b). The interface between the skin and foam showed well-joined morphology with a large amount of Si, as shown in Fig. 7(c). Regarding Si-infiltration, a fine Si powder with a mean particle size of 2 μm was also tested except for this coarse Si chip. However, the fine powder did not melt at 1550 °C because of its surface SiO_2 passivation layer, indicating the importance of the purity and size of Si particles for melt infiltration.

Fig. 8 shows the EDS results showing the composition of the different phases in the composite sample. The sample was composed of 3 different phases that could be distinguished with different contrasts. Based on the EDS results, the dark-gray, light-gray and black parts correspond to SiC, Si and carbon, respectively. The existence of a small amount of carbon was attributed to an incomplete reaction between the infiltrated Si and carbon black at 1550 °C. Fig. 9 shows XRD patterns of the SiC_f/SiC skin layer after Si-infiltration. The skin contained β-SiC, Si and SiO_2 with weight ratios of 81.4, 17.2 and 1.4 wt%, respectively, based on a Rietveld analysis, which corresponds to a volume ratio of 76.2, 21.2 and 1.6 vol.%. The existence of SiO_2 was attributed to the oxidation of Si and SiC surface. The skin also contained a small amount of carbon that was not detected by XRD because of low concentration, as explained above. The major phase existing in the final SiC_f/Si/SiC

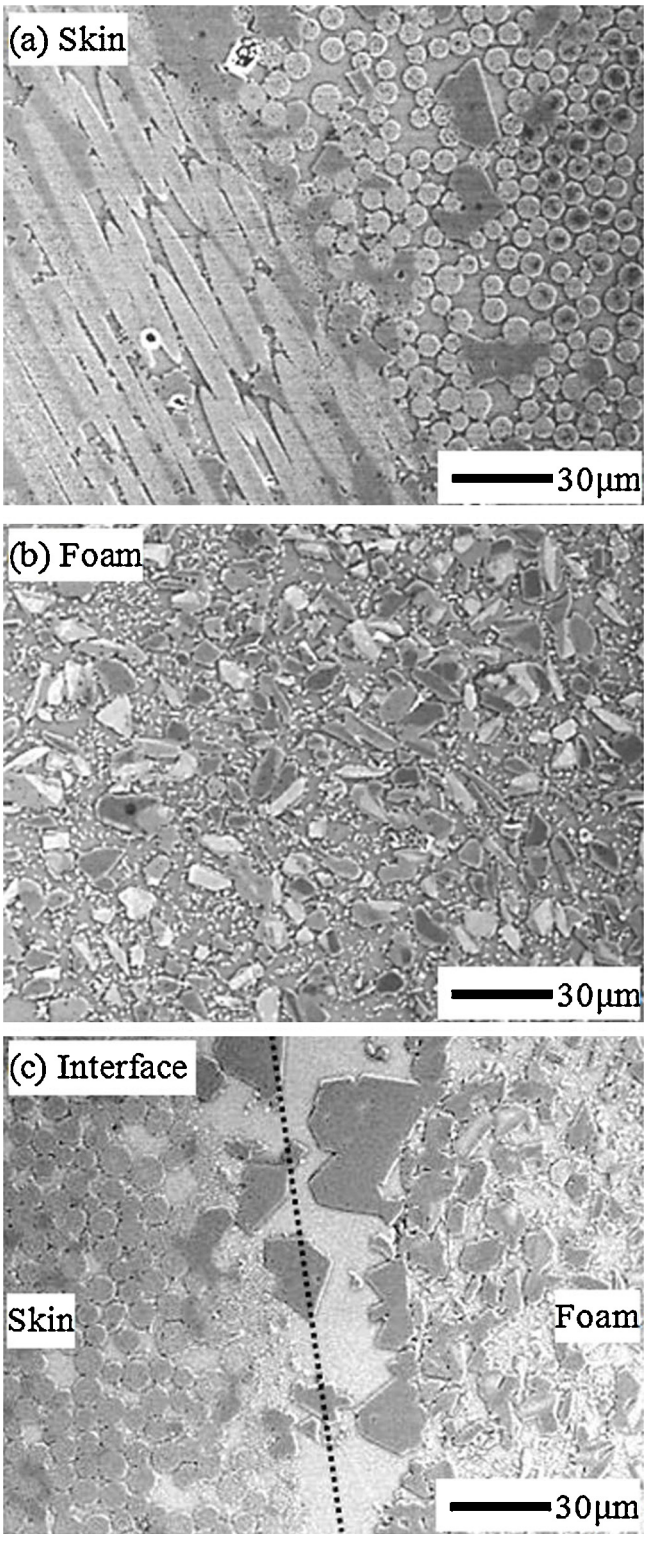

Fig. 7. SEM images of the polished surface of the sandwich-structured Si/SiC-based composite cylinders for (a) skin, (b) foam and (c) interface.

sample was SiC, which is desirable. Because of the higher thermal conductivity of SiC than of Si and SiO_2,[24–26] a larger portion of SiC is preferable. The β- to α-SiC transformation did not occur because 1550 °C was the highest temperature that the sample was exposed to. In addition, the skin layer revealed an

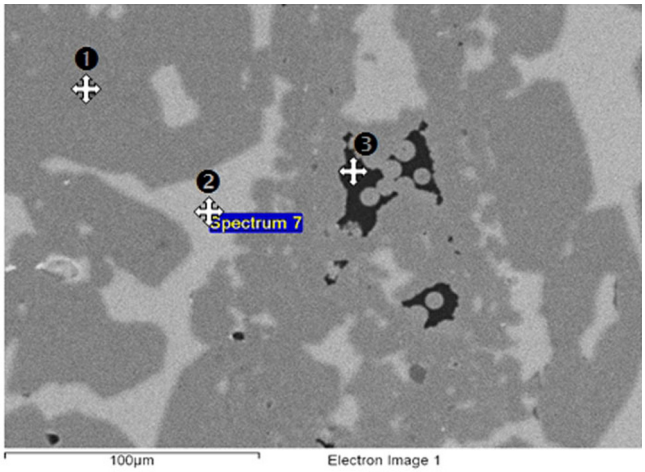

Element	Point 1 (at. %)	Point 2 (at. %)	Point 3 (at. %)
C K	49.83	0	99.80
Si K	50.17	100	0.20

Fig. 8. EDS analysis results for different points of the composite sample.

average flexural strength of 192.3 MPa based on 3-point bending test, while the final cylindrical sample showed gas tightness. Because Fend et al. demonstrated that SiC-based foams with high porosity showed the most desirable thermal transfer efficiency and absorptivity in the visible and near infrared range,[12] the cylindrical SiC_f/Si/SiC composite fabricated in this study is believed to improve the energy conversion efficiency compared to the conventional metal-based heat exchanger. Overall, the application of EPD followed by Si-infiltration is believed as an optimum method for the fabrication of a thin skin layer which possesses gas tightness as well as strength for high temperature heat exchanger applications, although further study is needed in optimizing the foam size and structure based on the thermophysical property evaluation for this sample, which is currently underway.

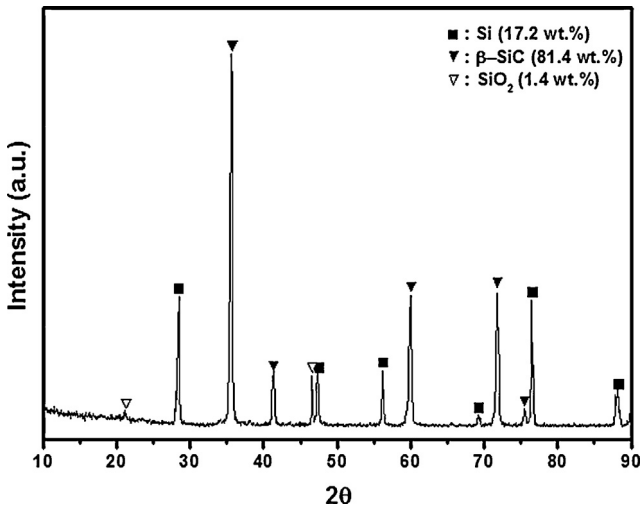

Fig. 9. XRD pattern of the sandwich-structured composite skin. The value in parenthesis indicates the % content of each phase based on a Rietveld simulation.

4. Conclusion

A cylindrical SiC-based composite was fabricated using a multi-step process for high temperature heat exchanger applications. After wrapping the Tyranno-SA3 SiC fabrics on a reticulated Si/SiC foam, the electrophoretic infiltration of SiC and carbon black matrix phase into the voids of the tubular SiC fabrics was performed. For the electrophoretic deposition, a stable slurry composed of ceramic particles, cationic dispersant and PVB binder was prepared by considering the zeta potential of ceramic constituents. The application of ultrasonic pulses during electrophoretic deposition at an operational pH of 4.0 in ethyl alcohol increased the degree of matrix particle infiltration into the deep voids of the SiC fabrics by minimizing the surface sealing effect. The composite sample exposed to the Si infiltration at 1550 °C revealed gas tightness owing to the highly dense skin microstructure and tightly connected foam-skin interface. The skin was composed of β-SiC, Si and SiO_2 at a volume ratio of 76.2, 21.2 and 1.6 vol.%, respectively, and showed an average flexural strength of 192.3 MPa.

Acknowledgements

This study was supported by the KORANET (www.koranet.eu) Joint Call on Green Technologies and by the Basic Science Research Program through the National Research Foundation of Korea (NRF) funded by the Ministry of Education, Science and Technology (Grant No. 2012000858). The authors wish to thank Mr. Gianella at Erbicol SA for providing the ERBISIC-R foam.

References

1. Sommers A, Wang Q, Han X, T'Joen C, Park Y, Jacobi A. Ceramics and ceramic matrix composites for heat exchangers in advanced thermal system – a review. *Appl Therm Eng* 2010;**30**:1277–91.
2. Dong S, Katoh Y, Kohyama A. Preparation of SiC/SiC composites by hot pressing, using Tyranno-SA fiber as reinforcement. *J Am Ceram Soc* 2003;**86**:26–32.
3. Yamada R, Taguchi T, Igawa N. Mechanical and thermal properties of 2D and 3D SiC/SiC composites. *J Nucl Mater* 2000;**283**(287):574–8.
4. Nannetti CA, Ortona A, de Pinto DA, Riccardi B. Manufacturing SiC-fiber – reinforced SiC matrix composites by improved CVI/slurry infiltration/polymer impregnation and pyrolysis. *J Am Ceram Soc* 2004;**87**:1205–9.
5. Margiotta JC, Zhang D, Nagle DC, Feeser CE. Formation of dense silicon carbide by liquid silicon infiltration of carbon with engineered structure. *J Mater Res* 2008;**23**:1237–48.
6. Yonathan P, Lee JH, Yoon DH, Kim WJ, Park JY. Improvement of SiCf/SiC density by slurry infiltration and tape stacking. *Mater Res Bull* 2009;**44**:2116–22.
7. Shin DW, Park SS, Choa YH, Niihara K. Silicon/silicon carbide composites fabricated by infiltration of a silicon melt into charcoal. *J Am Ceram Soc* 1999;**82**:3251–3.
8. Muňoz A, Martínz-Fernández J, Domíngues-Rodríguez A, Singh M. High-temperature compressive strength of reaction-formed silicon carbide (RFSC) ceramics. *J Eur Ceram Soc* 1998;**18**:65–8.
9. Boccaccini AR, Kaya C, Chawla KK. Use of electrophoretic deposition in the processing of fibre reinforced ceramic and glass matrix composites: a review. *Compos Part A* 2001;**32**:997–1006.
10. Besra L, Liu M. A review on fundamentals and applications of electrophoretic deposition (EPD). *Prog Mater Sci* 2007;**52**:1–61.
11. Gil GY, Yoon DH. Densification of SiC_f/SiC composites by electrophoretic infiltration combined with ultrasonication. *J Ceram Proc Res* 2011;**12**:371–5.
12. Fend T, Hoffschmidt B, Pitz-Paal R, Reutter O, Rietbrock P. Porous materials as open volumetric solar receivers: experimental determination of thermophysical and heat transfer properties. *Energy* 2004;**29**:823–33.
13. Ortona A, Pusterla S, Gianella S. An integrated assembly method of sandwich structured ceramic matrix composites. *J Eur Ceram Soc* 2011;**31**:1821–6.
14. Thirugnanasambandam M, Iniyan S, Goic R. A review of solar thermal technologies. *Renew Sust Energ Rev* 2010;**14**:312–22.
15. Müller-Steinhagen H, Trieb F. Concentrating solar power. *Ingenia* 2004;**18**:43–50.
16. Ishikawa T, Kohtoku Y, Kumegawa K, Yamamura T, Nagasawa T. High-strength alkali-resistant sintered SiC fibre stable to 2200 °C. *Nature* 1998;**391**:773–5.
17. Lee JH, Yonathan P, Yoon DH, Kim WJ, Park JY. Dispersion stability and its effect on tape casting of solvent-based SiC slurries. *J Ceram Process Res* 2009;**10**:301–7.
18. Yonathan P, Lee JH, Kim HT, Yoon DH. Properties of SiC_f/SiC composites fabricated by slurry infiltration and hot pressing. *Mater Sci Technol* 2011;**27**:257–63.
19. Barin I. *Thermochemical data of pure substances*. New York: VCH; 1989.
20. Chase Jr MW. *NIST-JANAF thermochemical tables*. 4th ed. New York: AIP; 1998.
21. Singh JP, Singh D, Sutaria M. Ceramic composites: roles of fiber and interface. *Compos Part A* 1999;**30**:445–50.
22. Shimoda K, Park JS, Hinoki T, Kohyama A. Influence of pyrolytic carbon interface thickness on microstructure and mechanical properties of SiC/SiC composites by NITE process. *Compos Sci Technol* 2008;**68**:98–105.
23. Ortona A, D'Angelo C, Gianella S, Gaia D. Cellular ceramics produced by rapid prototyping and replication. *Mater Lett* 2012;**80**:95–8.
24. Munro RG. Materials properties of a sintered α-SiC. *J Phys Chem Ref Data* 1997;**26**:1195–203.
25. Asheghi M, Touzelbaev MN, Goodson KE, Leung YK, Wong SS. Temperature-dependent thermal conductivity of single-crystal silicon layers in SOI substrates. *J Heat Trans-T ASME* 1998;**120**:30–6.
26. Hopkins PE, Kaehr B, Phinney LM, Koehler TP, Grillet AM, Dunphy D, Garcia F, Brinker CJ. Measuring the thermal conductivity of porous, transparent SiO_2 films with time domain thermoreflectance. *J Heat Trans-T ASME* 1998;**133**:061601–8.